

Evaluation of fusion splicing of hollow-core fibers to conventional single mode fiber

Mateusz Łukasz Józwicki,* Maciej Grzesiak, Paweł Mergo

Laboratory of Optical Fibers Technology, Maria Curie-Skłodowska University, Maria Curie-Skłodowska Sq. 5, 20-031, Lublin, Poland

Received November 26, 2025; accepted January 26, 2026; published March 31, 2026

Abstract—The paper presents the fusion splicing of a hollow-core fiber with a conventional single-mode fiber with the aim of preserving the internal hollow structure of the hollow-core fiber while achieving optimal mechanical strength and low optical loss at the splice. Each splice made at a different filament power was evaluated by measuring the power loss resulting from the splice, along with proof testing and visual inspection of the splice and the end face of the HCF after splice failure. The obtained results show a trade-off between power loss and splice strength. The highest splice strength was achieved at 16.0 W filament power, equal to 2.32 ± 0.09 N with the loss of 0.167 ± 0.011 dB, while the lowest loss of 0.010 ± 0.004 dB with splice strength of 0.22 ± 0.04 N was achieved at 13.0 W filament power.

Hollow-core optical fibers (HCFs) are a unique class of optical fibers in which light is guided primarily through an air-filled central core [1]. This approach potentially allows lower transmission losses and reduced nonlinear effects compared to conventional solid-core optical fibers. HCFs have attracted considerable interest for applications requiring low transmission loss, gas sensing [2], and ultrafast laser delivery systems [3].

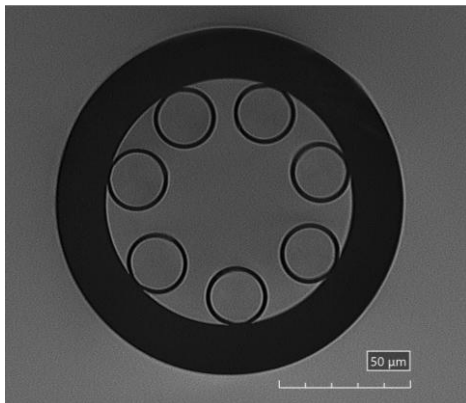


Fig. 1. Microscopic image of the HCF used for splicing.

One of the propagation mechanisms in hollow-core optical fibers involves guiding light via anti-resonant reflection from the thin walls of the cladding, which is usually made from capillaries. Splicing such fibers poses a significant challenge because it requires preserving the internal structure of the HCF [4–6]. A change in capillary

wall thickness shifts the spectral range of the light guided within the hollow core, which, in many cases, determines the performance of the experimental setup [7]. Table 1 summarizes some recent findings on the splicing of anti-resonant-propagation-based HCFs.

Table 1. Recent progress and findings in the field of HCF splicing

[3]	Splicing between an anti-reflection-coated solid-core fiber and HCF
[6]	Splicing of HCF to SMF with a reverse-tapering
[8]	Splicing between HCF and the solid end cap
[9]	SMF-HCF-SMF humidity sensor
[10]	Splicing of HCF to SMF through graded-index bridge fiber

The paper presents an evaluation of the splicing process of HCF with SMF by varying the filament power while keeping the remaining parameters unchanged. The main objective of varying the filament power was to determine the value at which the spliced HCF preserves the internal hollow-core structure while achieving optimal mechanical strength and minimal splice power loss. The achievement of such splices opens up broad possibilities for practical applications in precise measurement and experimental setups, where both high measurement accuracy and minimal optical losses are crucial. Splicing of the fibers was performed using a VYTRAN FFS2000 fusion splicer with a tungsten filament. Silica glass HCF used in the splicing process was manufactured in the Laboratory of Optical Fiber Technology UMCS at Lublin (Fig. 1), while SMF fiber was manufactured by OFS (AllWave® One). Geometrical parameters of the HCF are as follows: cladding diameter: 126.6 μm , core diameter: 48.3 μm , capillary wall thickness: 1.1 μm , capillary diameter: 19.5 μm , number of capillaries: 7.

Each splice was evaluated by measuring the power loss after each splice. The setup involved a superluminescent diode (SLD) light source (Thorlabs, S5FC1005P) coupled into an SMF used for splicing. Power at the HCF output was measured with a power meter (Thorlabs, PM100D) and an integrating-sphere photodiode (Thorlabs, S148C). Reference power before splicing was measured by positioning the optical fibers to be spliced as close as possible to their end faces. After the splice, power

* E-mail: mateusz.jozwicki@mail.umcs.pl



measurement was repeated, and the loss of power resulting from the splice was calculated from:

$$\text{Loss} = \left| 10 \log_{10} \left(\frac{P_1}{P_0} \right) \right| \quad (1)$$

where P_0 – power measured before splicing, P_1 – power measured after splicing.

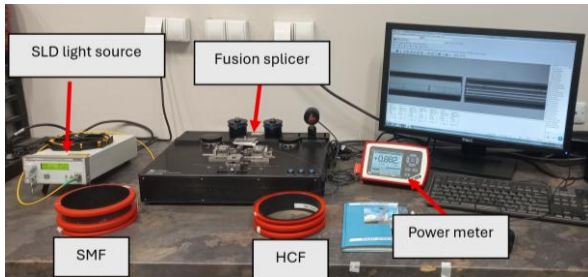


Fig. 2. Setup for fiber splicing and power measurement.

Each splice was subjected to proof testing using the integrated module of the fusion splicer and was tensioned to induce splice failure. The peak tensile force was set to 10 N and achieved within 20 s. The integrity of the internal structure of the HCF after the splice was checked by evaluating the side view of the splice and the end face of the HCF after each splice failure [11–12]. Splicing and testing at each filament power were repeated 5 times to check repeatability. The provided power loss uncertainty values refer to the uncertainty of the mean deviation. In contrast, the tensile strength measurement uncertainty represents a combined value that accounts for both the uncertainty of the mean deviation and the device's accuracy ($\pm 2\%$). The splicing setup is shown in Fig. 2.

Table 2. Initial parameters of the splicing process

Parameter	Value
Filament Power [W]	13.0 – 16.0 with a step of 1.0
Process Time [s]	3.0
Splice offset [μm]	0
Gap between fibers [μm]	8.0
Fiber push-in during process [μm]	6.0
Hot push [μm]	6.0
Delay before fiber push-in [s]	0.5
Argon flow [l/min]	0.95
Filament shift towards SMF [μm]	30

Initial parameters used in the fiber splicing process are presented in Table 2. Results of the splicing evaluation are shown in Tables 3 and 4. Average values of the results are shown in Fig. 3. Increasing filament power results in the increase of power loss after splicing up to 0.167 ± 0.011 dB at 16.0 W. Lowest loss of 0.010 ± 0.004 dB is obtained at filament power of 13.0 W. Still, such

low power results in weak splice strength 0.22 ± 0.04 N. Highest splice strength has been obtained at filament power of 16.0 W and is equal to 2.32 ± 0.09 N. For comparison, the splice strength between HCF and SMF reported in [4] is 140 g (1.37N). Comparable splice strength of 1.98 ± 0.10 N has been obtained with filament power of 15.0 W, at which power loss was equal to 0.077 ± 0.007 dB. Such low loss is rather acceptable in most cases.

Table 3. Loss introduced after the splicing fibers at different filament powers

Filament power [W]	13.0	14.0	15.0	16.0
Sample 1	0.013 dB	0.017 dB	0.093 dB	0.162 dB
Sample 2	0.005 dB	0.026 dB	0.085 dB	0.150 dB
Sample 3	0.005 dB	0.027 dB	0.051 dB	0.154 dB
Sample 4	0.023 dB	0.016 dB	0.077 dB	0.212 dB
Sample 5	0.004 dB	0.030 dB	0.081 dB	0.159 dB
Average	0.010 dB	0.023 dB	0.077 dB	0.167 dB
Uncertainty	0.004 dB	0.003 dB	0.007 dB	0.011 dB

Table 4. Failure force of the splice at different filament powers

Filament power [W]	13.0	14.00	15.00	16.00
Sample 1	0.3 N	0.9 N	1.9 N	2.3 N
Sample 2	0.2 N	0.8 N	1.8 N	2.2 N
Sample 3	0.3 N	1.1 N	1.9 N	2.4 N
Sample 4	0.1 N	1.0 N	2.2 N	2.4 N
Sample 5	0.2 N	0.9 N	2.1 N	2.3 N
Average	0.22 N	0.94 N	1.98 N	2.32 N
Uncertainty	0.04 N	0.06 N	0.10 N	0.09 N

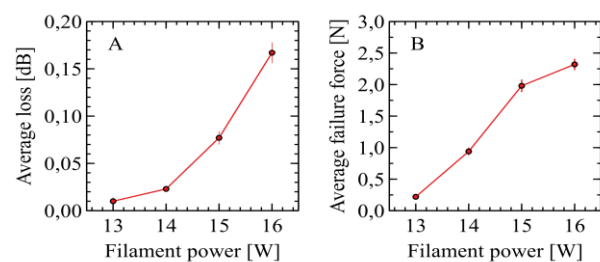


Fig. 3. Average power loss after splice (A) and average failure force of the splice (B) depending on the filament power during splicing.

Besides evaluating power loss after the splice it is important to check internal hollow structure of the HCF after each splice. Images showing the side views of the splices obtained at different filament power are shown on Fig. 4. At filament power of 13.0 W and 14.0 W no significant structure change is seen. As discussed before, those splices do not introduce much loss but result in low splice strength. At a higher filament power of 15.0 W,

slight irregularities are observed near the splice. At the highest power of 16.0 W, deformations are more pronounced. Figure 5 shows the end faces of HCF after each splice has been tested for failure. Similarly to side views, the end faces of the HCF after splicing at 13.0 and 14.0 W filament power show no distinct change, with their internal capillary diameters being 19.3 and 19.1 μm , respectively. Compared to a non-heat-treated fiber, in which the capillary internal diameter was 19.5 μm . At higher filament power, capillary collapse is more pronounced, as evidenced by the deviation from a round shape and by their internal diameters of 17.5 and 14.7 μm , respectively.

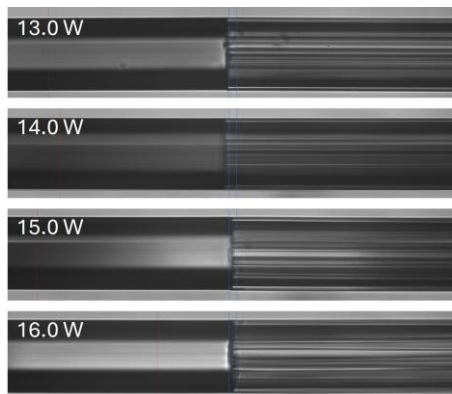


Fig. 4. Side view of the splices at different filament powers.

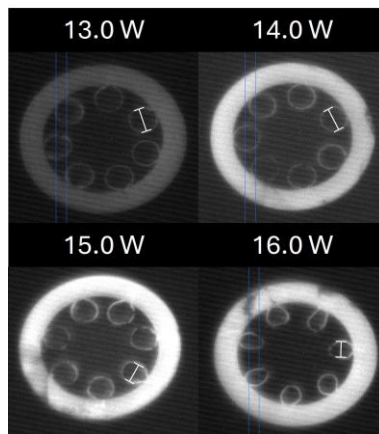


Fig. 5. End view of the HCF after splice failure obtained at different filament powers.

The obtained results suggest that there is a high possibility of obtaining low-loss splices with good mechanical strength between used HCF and SMF. Although at higher filament power (15.0–16.0 W) the capillary structure of the HCF near the splice is not maintained, the obtained loss is relatively low (0.167 ± 0.011 dB). It is important to note that in our case, there is almost a fivefold difference between the core diameters of the SMF and the HCF. In this case, the internal structure of capillaries near the splice may not be

as important if the spliced fibers had similar core sizes. Additionally, our power-loss measurement method evaluated only the impact of splice parameters on output power. The extended evaluation should include power loss due to MFD mismatch and HCF attenuation. Also, analysis of the splice between SMF and HCF, where light is coupled from HCF into SMF, would be advisable as the next experiment.

Reported results indicate the possibility of making low-loss splices between HCF and SMF. Those results pave the way for future work on the development of low-loss splices between two HCF fibers, which will require significantly greater precision and accuracy to preserve propagation in the hollow, air-core. The choice of splicing parameters is dictated by the specific application requirements, particularly the relative emphasis on achieving high mechanical strength versus minimizing optical losses. In practice, this involves an explicit trade-off between maximizing the tensile reliability of the splice at the cost of increased loss, or, alternatively, optimizing optical performance while accepting a reduction in splice robustness.

This work was supported by the infrastructure of National Laboratory for Photonics and Quantum Technologies (POIR.04.02.00-00-B003/18-00) which has been used for the manufacturing of the optical fibers and their characterization.

References

- [1] M.S. Habib, J.E. Antonio-Lopez, C. Markos, A. Schülzgen, R. Amezcua-Correa, *Opt. Expr.* **27**, 3824 (2019); <https://doi.org/10.1364/OE.27.003824>
- [2] P. Jarowski, *Sensors* **21**, 5640 (2021); <https://doi.org/10.3390/s21165640>
- [3] J. Shi, *et al.*, *Nat. Commun.* **16**, 8965 (2025); <https://doi.org/10.1038/s41467-025-64073-y>
- [4] Y. Min *et al.* *J. Lightwave Technol.* **39**, 3251 (2021); <https://doi.org/10.1109/JLT.2021.3058888>
- [5] R. Thapa, K. Knabe, K.L. Corwin, B.R. Washburn, *Opt. Expr.* **14**, 9576 (2006); <https://doi.org/10.1364/OE.14.009576>
- [6] C. Wang, *et al.*, *Opt. Expr.* **29**, 22470 (2021); <https://doi.org/10.1364/OE.432147>
- [7] F. Poletti, *Opt. Expr.* **22**, 23807 (2014); <https://doi.org/10.1364/OE.22.023807>
- [8] J. Shi, X. Ye, Y. Cui, W. Huang, H. Li, Z. Zhou, *et al.*, *Photonics* **8**, 371 (2021); <https://doi.org/10.3390/photonics8090371>
- [9] A. Cheng, C. Wang, J. Xu, P. Zhang, Y. Zheng, S. Dai, *Photon. Sens.* **15**, 250202 (2025); <https://doi.org/10.1007/s13320-025-0749-1>
- [10] Z. Zhang, R. Li, C. Wang, M. Zhou, Y. Liu, Y. Pang, *J. Opt. Technol.* **90**, 42 (2023); <https://doi.org/10.1364/JOT.90.000042>
- [11] A.D. Yablon, R.T. Bise, *IEEE Photon. Techn. Lett.* **17**, 180120 (2005); <https://doi.org/10.1109/LPT.2004.838153>
- [12] M. Murawski, L.R. Jaroszewicz, K. Stasiewicz *Phot. Lett. Poland* **1**, 115 (2009); <https://doi.org/10.4302/photon.%20lett.%20pl.v1i3.60>